Charge-transfer spectroscopy and photochemistry of alkylamine cobalt(III) complexes*

Scott K. Weit[a], Guillermo Ferraudi[b], Paul A. Grutsch[a] and Charles Kutal[a]
[a]*Department of Chemistry, The University of Georgia, Athens, GA 30602 (USA)*
[b]*Radiation Laboratory, University of Notre Dame, Notre Dame, IN 46556 (USA)*

(Received 2 November 1992)

CONTENTS

ABSTRACT

Spectroscopic and photochemical studies are reported for $Co(NH_2R)_6^{3+}$, $Co(NH_2R)_5OH_2^{3+}$, and $Co(NH_2R)_5X^{2+}$ (where R is methyl, ethyl, or *n*-propyl, and X is Cl^- or Br^-). These complexes absorb strongly in the ultraviolet region owing to the presence of one or more ligand-to-metal charge transfer (LMCT) band(s). Irradiation into this charge transfer region results in redox decomposition of the complex with the release of Co^{2+}, alkylamine, and a radical. Photoredox quantum yields measured in fluid solution are generally high and dependent upon excitation wavelength, oxygen concentration, temperature, and solution viscosity. In contrast to their well-studied ammine analogues, the alkylamine complexes (1) possess a N→Co charge transfer band at wavelengths well above 200 nm, (2) undergo redox decomposition from the X→Co *and* N→Co charge transfer excited states, and (3) avoid an intermolecular decomposition pathway involving photooxidation of the solvent. Reasons for these differences between the two families of complexes are discussed.

* Dedicated to the memory of John C. Bailar, Jr., an exceptional teacher, scientist, and human being.
Correspondence to: C. Kutal, Department of Chemistry, The University of Georgia, Athens, GA 30602, USA.

0010-8545/93/$24.00

1. INTRODUCTION

Ligand-to-metal charge transfer (LMCT) excited states of coordination compounds exhibit a rich, redox-based chemistry [1–5]. Exemplary in this respect are complexes belonging to the $Co(NH_3)_5X^{2+}$ family, where X is a uninegative ligand such as Cl^-, Br^-, N_3^-, NO_2^-, or NCS^-. Irradiation of the X→Co charge transfer (CT) absorption band induces efficient redox decomposition accompanied, in many cases, by ligand substitution and/or linkage isomerization. Early models attributed such behavior to the reactivity of either the LMCT excited state or a successor radical pair, but the weight of evidence now supports the view that both types of species play important roles. Thus the X→Co CT state initially populated upon light absorption can undergo non-reactive relaxation to the ground state in competition with homolytic scission of the Co–X bond to generate a primary (solvent-caged) radical pair (eqn. (1); an asterisk denotes an electronic excited state). This primary pair can either reform the parent complex (eqn. (2)) or diffuse apart to produce a secondary (solvent-separated) radical pair (eqn. (3); S denotes a solvent molecule). The secondary radical pair, in turn, can recombine to form the original complex or perhaps an isomer (eqn. (4)), or diffuse apart with (eqn. (5)) or without (eqn. (6)) back-electron transfer to X. The substitutionally labile $Co(NH_3)_5^{2+}$ fragment produced in eqn. (6) undergoes rapid and irreversible loss of NH_3 to yield solvated Co^{2+} (eqn. (7)) [6].

$$[(NH_3)_5Co^{III}X]^{2+} \xrightarrow{h\nu} [(NH_3)_5Co^{III}X]^{2+*} \longrightarrow \{(NH_3)_5Co^{II}, X\cdot\}^{2+}_{\text{solvent cage}} \quad (1)$$

$$\{(NH_3)_5Co^{II}, X\cdot\}^{2+} \longrightarrow [(NH_3)_5Co^{III}X]^{2+} \quad (2)$$

$$\{(NH_3)_5Co^{II}, X\cdot\}^{2+} \longrightarrow [(NH_3)_5Co^{II}S]^{2+}, X\cdot \quad (3)$$

$$[(NH_3)_5Co^{II}S]^{2+}, X\cdot \longrightarrow [(NH_3)_5Co^{III}X]^{2+} \quad (4)$$

$$[(NH_3)_5Co^{II}S]^{2+}, X\cdot \longrightarrow [(NH_3)_5Co^{III}S]^{3+} + X^- \quad (5)$$

$$[(NH_3)_5Co^{II}S]^{2+}, X\cdot \longrightarrow [(NH_3)_5Co^{II}S]^{2+} + X\cdot \quad (6)$$

$$[(NH_3)_5Co^{II}S]^{2+} \rightarrow Co^{2+}_{(solv)} + 5NH_3 \quad (7)$$

According to this mechanism, the quantum yield of photoredox decomposition, $\phi_{Co^{2+}}$, can be expressed by eqn. (8), where ϕ_{RP} is the efficiency of forming the primary radical pair in eqn. (1), and the rate constants k_2–k_6 refer to the processes described by eqns. (2)–(6), respectively. A drop in $\phi_{Co^{2+}}$ with increasing solvent viscosity is expected and often observed, since the rates at which the primary (eqn. (3)) and secondary (eqn. (6)) radical pairs diffuse apart should decrease in viscous media.

Given the complex nature of the photoredox process, however, it is not surprising that characteristics of the solvent (e.g. dielectric properties, hydrogen-bonding ability, basicity) other than viscosity can influence the value of $\phi_{Co^{2+}}$ [7–9].

$$\phi_{Co^{2+}} = \phi_{RP}\left(\frac{k_3}{k_2 + k_3}\right)\left(\frac{k_6}{k_4 + k_5 + k_6}\right) \tag{8}$$

Redox decomposition also results from irradiation of the higher-energy N→Co CT absorption band. For $Co(NH_3)_5X^{2+}$ (X = Cl^-, Br^-, or N_3^-) in aqueous solution, this process occurs with a quantum efficiency identical to that measured for direct X→Co CT excitation [2,3]. Such behavior suggests that the N→Co CT excited state can relax with near unit efficiency to the X→Co CT state, which then initiates the sequence of reactions described by eqns. (1)–(7). The alternative explanation requiring the two states in each complex to undergo redox decomposition with equal $\phi_{Co^{2+}}$ values seems less plausible.

Very different behavior has been observed in mixed-solvent systems, where a steep rise in $\phi_{Co^{2+}}$ at short excitation wavelengths signals the occurrence of a new photoredox process. Endicott and co-workers [10] proposed that the N→Co CT excited state can cross to a dissociative CT state arising from the transfer of an electron from a solvent molecule to the complex (eqn. (9)). It was further suggested that this intermolecular process, which leads to the formation of a solvent radical in the primary photochemical step, is reasonably general for deep-ultraviolet excitations of coordination complexes.

$$\{(NH_3)_5Co^{III}X^{2+}, H_2O\} \xrightarrow{h\nu} \{(NH_3)_5Co^{II}X^{+}, H_2O^{+\cdot}\}^*$$

$$\rightarrow Co^{2+}_{(solv)} + 5NH_3 + X^- + H_2O^{+\cdot} \tag{9}$$

Our efforts to discover new classes of base-releasing inorganic photoinitiators for microimaging and curing applications [11–13] led us to investigate the LMCT spectroscopy and photochemistry of $Co(NH_2Me)_6^{3+}$, $Co(NH_2R)_5OH_2^{3+}$, and $Co(NH_2R)_5X^{2+}$, where R is methyl (Me), ethyl (Et), or *n*-propyl (Pr), and X is Cl^- or Br^- [14,15]. While ultraviolet irradiation of these complexes in solution causes photoredox decomposition, the mechanism differs in some key respects from that described above (eqns. (1)–(7) and (9)) for the $Co(NH_3)_5X^{2+}$ family. In particular, the alkylamine complexes undergo intramolecular redox reactions from both the X→Co and N→Co CT excited states. Furthermore, the intermolecular redox process involving the direct participation of solvent (analogous to eqn. (9)) appears to be unimportant. These differences and their mechanistic implications form the subject of this article.

2. EXPERIMENTAL SECTION

2.1 Reagents and equipment

Literature procedures were followed in the syntheses of $[Co(NH_2Me)_6]Br_3$ [16], $[Co(NH_2Me)_5Cl](ClO_4)_2$ [17] (obtained from the chloride salt by two recrystallizations from aqueous $HClO_4$–$NaClO_4$ solution), $[Co(NH_2Me)_5Br](ClO_4)_2$, [18] $[Co(NH_2Et)_5Cl]Cl_2$ [19], $[Co(NH_2Pr)_5Cl]Cl_2$ [19,20], and $[Co(NH_2Pr)_5OH_2](ClO_4)_3$ [20]. **Caution:** perchlorate salts are potentially explosive if subjected to heating or mechanical shock. Excellent elemental analyses were obtained for the methylamine complexes, whereas the results were somewhat less satisfactory for the ethylamine and *n*-propylamine complexes (Table 1). Since we were unable to isolate $Co(NH_2Me)_5OH_2^{3+}$ as a solid salt, studies of this complex were conducted on solutions of fully aquated (as determined by electronic spectroscopy) $Co(NH_2Me)_5Cl^{2+}$. Distilled water, acetonitrile (Burdick and Jackson spectral grade), methanol (Baker HPLC grade), and glycerol (Baker reagent grade) were used as solvents in the spectral and photochemical experiments. Solutions of the complexes contained 10^{-3} M $HClO_4$ to prevent base hydrolysis.

Electronic absorption spectra were recorded on Cary 219 and Varian DMS 300 spectrophotometers. Fluorescence measurements were taken with a Perkin Elmer MPF-44B spectrofluorimeter. Hydrogen ion concentration was determined with a Fisher AccupHast combination pH microelectrode and a Corning digital 112 pH meter. Continuous photolyses at selected wavelengths above 254 nm were performed with a 200 W high-pressure mercury-arc lamp in conjunction with a high-intensity monochromator, while low-pressure mercury, cadmium, and zinc lamps were employed for excitations at 254, 229, and 214 nm, respectively. Incident light intensities at wavelengths $\geqslant$254 nm were determined by ferrioxalate actinometry [21], whereas

TABLE 1

Elemental analysis data for (alkylamine)cobalt(III) complexes

Complex	Analysis (calcd.)[a]		
	C (%)	H (%)	N (%)
$[Co(NH_2Me)_6]Br_3$	14.85(14.86)	6.37(6.23)	—
$[Co(NH_2Me)_5Cl](ClO_4)_2$	18.94(18.73)	7.85(7.86)	22.22(21.85)
$[Co(NH_2Me)_5Br](ClO_4)_2$	12.33(12.18)	5.19(5.10)	13.86(14.20)
$[Co(NH_2Et)_5Cl]Cl_2$[b]	30.01(30.74)	9.03(9.03)	17.77(17.92)
$[Co(NH_2Pr)_5Cl]Cl_2$[b]	38.28(39.09)	9.64(9.84)	14.85(15.19)
$[Co(NH_2Pr)_5OH_2](ClO_4)_3$[b]	26.25(26.85)	7.06(7.06)	10.13(10.43)

[a]Analyses were performed by Galbraith Laboratories, Knoxville, TN.

[b]Complex was kept in a desiccator under continuous vacuum for two days. Samples not subjected to this treatment gave very poor analyses.

the redox decomposition of $Co(NH_3)_5Cl^{2+}$ in aqueous solution [3] served as a convenient actinometer at shorter wavelengths.

Since the apparatus employed in the flash photolysis experiments has been described previously [22], only a few salient features will be summarized here. Pulses of polychromatic light having a duration of ~ 30 μs were obtained from two FP 8-100C flash lamps (Xenon Corp.) fired simultaneously. The desired excitation wavelength region was isolated by means of a solution cut-off filter (60 g KNO_3 in 300 ml of water for >250 nm; 10% KBr in water for >240 nm). Photogenerated transients were detected optically with an analyzing light beam directed through the sample cell.

2.2 Photochemical studies

In a typical photochemical experiment, a 3 ml aliquot of the sample solution was pipetted into a 1 cm rectangular quartz cell and a small magnetic stirring bar added to provide continuous agitation during photolysis. The cell was capped, placed in a thermostatted holder, and its contents allowed to equilibrate at the desired temperature for 15 min. In some runs, the sample solution was bubbled with argon during this equilibration period to remove dissolved oxygen.

Photolyzed solutions were analyzed for Co^{2+} by a modification of the method of Vydra and Pribil [23]. In brief, a 2 ml aliquot of the photolyte was pipetted into a 10 ml volumetric flask containing 2 ml of an acidified 2.2×10^{-3} M ferric chloride solution, 3 ml of acidified 0.6 M sodium acetate solution, and 3 ml of a 0.1% solution of 1,10-phenanthroline. The resulting solution was stirred in the dark for 20 min and its absorbance measured at 510 nm. A similar procedure was performed on a non-irradiated sample to provide a blank value. A previously constructed calibration curve was used to convert absorbance readings to Co^{2+} concentrations. Photolyzed solutions subject to analysis for free amine were passed through a column packed with 1–1.5 ml of Chelex 100 cation exchange resin (Bio Rad). This procedure removed multiply charged cobalt-containing species while allowing elution of the amine with 10^{-3} M $HClO_4$. The eluant was treated with fluorescamine reagent and the amine concentration determined fluorimetrically by the procedure of Udenfriend and co-workers [24]. Quantitative analysis of formaldehyde in the photolyte was achieved by the method of Schmidt et al. [25].

3. RESULTS AND DISCUSSION

3.1 Spectral studies

Each of the alkylamine complexes examined in this study possesses one or more intense absorption bands in the ultraviolet region. Table 2 summarizes spectral data for several complexes in acidified aqueous solution, while Figs. 1–3 display the actual spectra of $Co(NH_2Me)_5OH_2^{3+}$, $Co(NH_2Me)_5Cl^{2+}$, and $Co(NH_2Me)_5Br^{2+}$,

TABLE 2

Charge-transfer spectral data for (alkylamine)cobalt(III) complexes[a]

Complex	$10^{-3}\,\nu_{max}$(calcd.), cm^{-1}[b]	$10^{-3}\,\nu_{max}$(obs.), cm^{-1} ($10^{-3}\,\varepsilon$, $M^{-1}\,cm^{-1}$)	Assignment
$Co(NH_2Me)_6^{3+}$	45.12	44.44(31.0)	$N \rightarrow Co$
$Co(NH_2Me)_5Cl^{2+}$	43.55	42.28[c](26.6)	$N \rightarrow Co$
	41.15		$Cl(\sigma) \rightarrow Co$[d]
$Co(NH_2Et)_5Cl^{2+}$	43.35	41.87[c](28.8)	$N \rightarrow Co$
	40.95		$Cl(\sigma) \rightarrow Co$[d]
$Co(NH_2Pr)_5Cl^{2+}$	43.38	41.25[c](30.2)	$N \rightarrow Co$
	40.98		$Cl(\sigma) \rightarrow Co$[d]
$Co(NH_2Me)_5Br^{2+}$	43.07	44.51(18.1)	$N \rightarrow Co$
	36.77	37.85(18.0)	$Br(\sigma) \rightarrow Co$[d]
	29.87	29 (sh)	$Br(\pi) \rightarrow Co$[d]
$Co(NH_2Me)_5OH_2^{3+}$	53.34	[e]	$O \rightarrow Co$
	44.34	44.05(25.0)	$N \rightarrow Co$
$Co(NH_2Pr)_5OH_2^{3+}$	53.06	[e]	$O \rightarrow Co$
	44.06	41.84(28.0)	$N \rightarrow Co$

[a]Measured at 10.0°C in water acidified to pH ~ 3.2 with $HClO_4$.

[b]Calculated by using eqn. (10) and parameters taken from the following sources: χ_L and χ_M from refs. 2 and 5; Dq from ref. 18 and Dq, B, and C from ref. 34. The spin-pairing term, δSP, was calculated from the expression $-7/6[(5/2)B + C]$, where B and C are the Racah parameters.

[c]Overlapping of $N \rightarrow Co$ and $Cl(\sigma) \rightarrow Co$ CT absorption bands occurs.

[d]σ (or π) designates an electron in an orbital having σ- (or π-) symmetry with respect to the metal–ligand bond.

[e]Transition lies outside of the detection range of spectrophotometer.

respectively. The absorption bands can be confidently assigned as LMCT in character based upon a comparison of the observed transition energies with those calculated from the Jorgensen semiempirical relation (eqn. (10)) [2,5,26].

$$\nu_{max} = 30(\chi_L - \chi_M) + 10Dq + \delta SP \tag{10}$$

In this expression, ν_{max} is the band maximum, χ_L and χ_M represent the optical electronegativities of the ligand and metal, respectively, that undergo charge transfer, Dq is the ligand field strength parameter, and δSP denotes the difference in spin-pairing energy between the ground and excited states involved in the transition. Substitution of the appropriate parameters into the right side of the expression yields the calculated transition energies listed in column 2 of Table 2. The experimentally observed energies appear in column 3, while column 4 lists our transition assignments. The generally good agreement between the calculated and observed ν_{max} values leaves little doubt that these transitions occur with a substantial degree of LMCT character.

Table 3 lists the LMCT absorption maxima for $Co(NH_2Me)_5Br^{2+}$ and

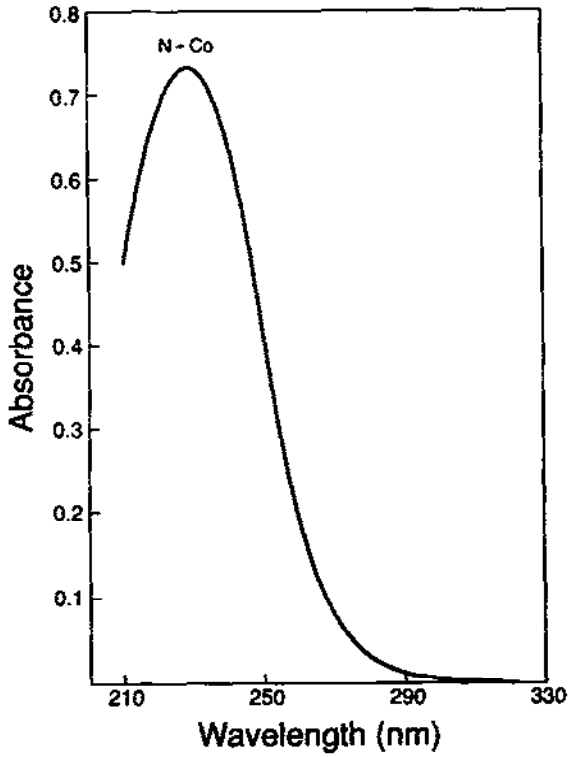

Fig. 1. Ultraviolet absorption spectrum of $Co(NH_2Me)_5OH_2^{3+}$ in pH ~3 $HClO_4$ at 10°C.

$Co(NH_3)_5Br^{2+}$ in several solvents. Switching from water (dielectric constant 78.5) to the less polar glycerol (42.5), acetonitrile (36.2), or methanol (32.6) lowers the energy of the Br→Co CT transition by similar increments (ΔE) for the two complexes. This red shift arises from the different charge distributions in the ground and excited states. As depicted by the simplified structure in eqn. (11),

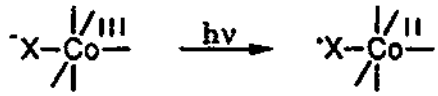

(11)

polar ground state **less polar excited state**

the charge transfer transition causes an inward flow of electron density that decreases the dipole moment of the complex. Changing to a less polar solvent destabilizes the ground state (decreases its solvation energy) more than the excited state and thus lowers the transition energy. Solvent polarity arguments, however, do not explain the finding that the N→Co CT transition in $Co(NH_2Me)_5Br^{2+}$ experiences a red shift (relative to water) in hydroxylic solvents (50% glycerol, methanol) and a blue

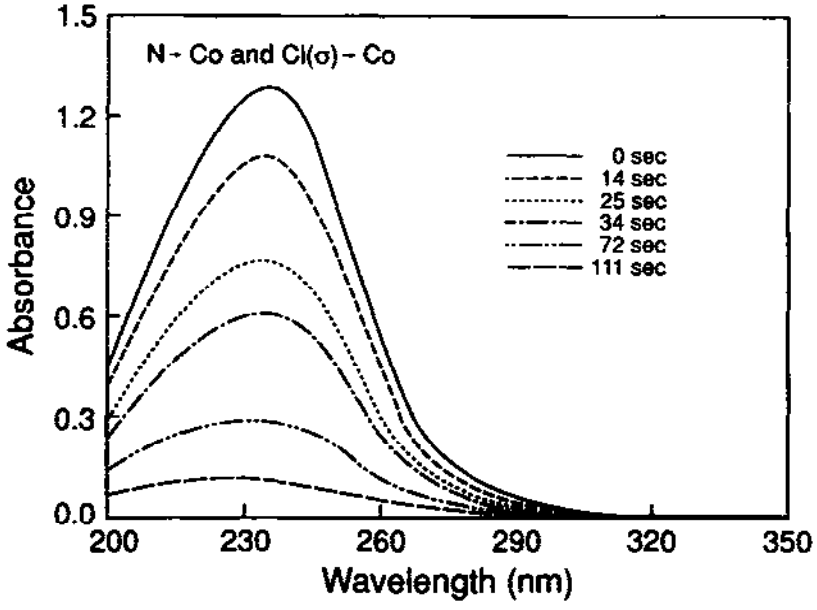

Fig. 2. Bleaching of the ultraviolet absorption band of $Co(NH_2Me)_5Cl^{2+}$ in pH ~3 $HClO_4$ at 10°C as a function of time of irradiation at 254 nm. Zero-time spectrum corresponds to unirradiated complex.

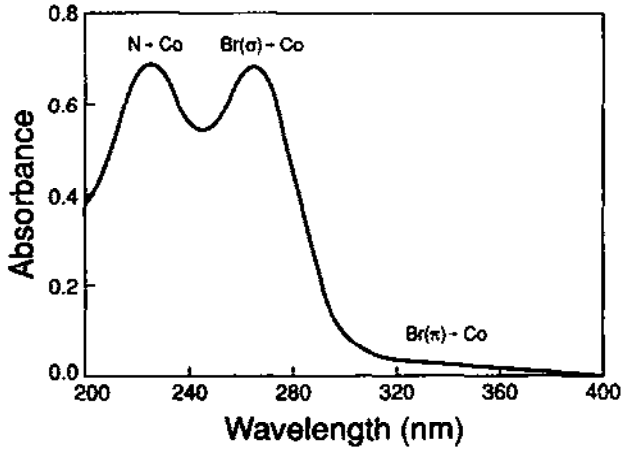

Fig. 3. Ultraviolet absorption spectrum of $Co(NH_2Me)_5Br^{2+}$ in pH ~3 $HClO_4$ at 10°C.

shift in predominantly non-hydroxylic media (80% CH_3CN, CH_3CN). A specific association between the complex and solvent must be involved, and we have proposed a hydrogen-bonding interaction of the type described by eqn. (12) [15]. The increased positive charge on the amine nitrogen atoms that results from N → Co CT enhances the acidity of the directly attached hydrogen atoms. Consequently, electron-

TABLE 3

LMCT spectral data for cobalt(III) complexes in different solvents[a]
Reproduced from ref. 15. Copyright 1991 American Chemical Society

Solvent[c]	$Co(NH_3)_5Br^{2+}$		$Co(NH_2Me)_5Br^{2+}$			
	$Br(\sigma) \rightarrow Co$[b]		$Br(\sigma) \rightarrow Co$		$N \rightarrow Co$	
	ν_{max}[d]	ΔE[e]	ν_{max}[d]	ΔE[e]	ν_{max}[d]	ΔE[e]
H_2O	39.52	0.00	37.87	0.00	44.52	0.00
50% Glycerol	39.31	0.21	37.59	0.28	44.36	0.16
>99.9% CH_3OH	38.96	0.56	37.40	0.47	44.06	0.46
80% CH_3CN	39.35	0.17	37.59	0.28	44.74	−0.22
>99.9% CH_3CN	38.90	0.62	37.54	0.33	45.14	−0.62

[a]Measured at 10.0 ± 0.5°C in solvents containing 10^{-3} M $HClO_4$.
[b]σ refers to an electron in an orbital having σ-symmetry with respect to the metal–ligand bond.
[c]Water is the other component in the mixed-solvent systems.
[d]Energy of absorption maximum; units are 10^3 cm^{-1}. Estimated accuracy is 70–100 cm^{-1}.
[e]Difference between ν_{max} values measured in water and the indicated solvent; units are 10^3 cm^{-1}.

pair donation from a solvent molecule to one of these hydrogens should be greater in the excited state than in the ground state, and this added stabilization causes the $N \rightarrow Co$ CT transition to move to lower energy as the Lewis basicity of the solvent increases (acetonitrile < water < methanol).

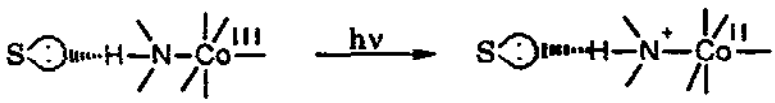

(12)

Several other features of the LMCT spectra of cobalt(III) alkylamine complexes should be noted. The $N \rightarrow Co$ CT transition generally occurs at an energy $\sim 5 \times 10^3$ cm^{-1} below that found for the corresponding ammine complex owing to the smaller χ_L and Dq values of NH_2R versus NH_3. The smaller Dq also results in lower energies for the $X \rightarrow Co$ CT transitions. The single absorption band observed in the spectrum of $Co(NH_2R)_5OH_2^{3+}$ (Fig. 1) corresponds to the $N \rightarrow Co$ CT transition; the $O \rightarrow Co$ CT transition occurs at appreciably higher energy (Table 2) and thus falls outside the detection range of our spectrophotometer. For the series of $Co(NH_2R)_5Cl^{2+}$ complexes, the $N \rightarrow Co$ and $Cl(\sigma) \rightarrow Co$ CT transitions lie sufficiently close in energy to form a single, composite absorption band (Fig. 2). Only $Co(NH_2Me)_5Br^{2+}$ exhibits distinct LMCT bands in the experimentally accessible wavelength region (Fig. 3). This characteristic makes the bromo complex especially well-suited for studies probing the extent of communication between different LMCT excited states.

3.2 Photochemical studies

Continuous ultraviolet irradiation of a cobalt(III) alkylamine complex in acidic aqueous solution causes a steady decrease in the intensity of its LMCT absorption band(s) (e.g. Fig. 2). This bleaching results from the photoredox decomposition of the complex to Co^{2+}, free alkylamine, and a radical. Mechanistic studies reveal that the quantum efficiency and stoichiometry of the photochemical reaction can be influenced by several factors including excitation wavelength, presence of oxygen, and temperature. In interpreting this behavior, it will be convenient to divide the complexes into three groups: (a) $Co(NH_2Me)_6^{3+}$ and $Co(NH_2R)_5OH_2^{3+}$; (b) $Co(NH_2Me)_5Br^{2+}$; and (c) $Co(NH_2R)_5Cl^{2+}$. The photoreactivity patterns within each group can then be correlated with the type of LMCT excited state initially populated upon light absorption.

3.2.1 $Co(NH_2Me)_6^{3+}$, $Co(NH_2Me)_5OH_2^{3+}$, and $Co(NH_2Pr)_5OH_2^{3+}$

Irradiation of $Co(NH_2Me)_6^{3+}$ in its N→Co CT region induces efficient redox decomposition. The quantum efficiency, $\phi_{Co^{2+}}$, is independent of excitation wavelength and temperature, but decreases sharply in the presence of oxygen (Table 4). We attribute the latter effect to the reactivity of the $\cdot^{+}NH_2Me$ cation radical generated in the primary photochemical step (eqn. (13)) [27]. Deprotonation of this species affords the corresponding uncharged radical, $\cdot NH_2CH_2$, which, in deoxygenated solution, can reduce the parent complex (eqn. (14)). Scavenging of the nitrogenous radicals by O_2 inhibits this thermal redox process and thereby lowers $\phi_{Co^{2+}}$. The relative contribution of the photochemical and thermal pathways for Co^{2+}

TABLE 4
Photoredox quantum yield data for $Co(NH_2Me)_6^{3+}$ and $Co(NH_2R)_5OH_2^{3+}$

Complex	λ_{excit} (nm)	Temp. (°C)	$\phi_{Co^{2+}}$[a]	
			Ar purged	Air-saturated
$Co(NH_2Me)_6^{3+}$	254	5	0.73 ± 0.06[b]	—[c]
	254	10	0.70 ± 0.03	0.45 ± 0.03
	254	25	0.73 ± 0.01	0.46 ± 0.03
	229	5	0.75 ± 0.01	—
	229	10	0.70 ± 0.07	0.46 ± 0.01
	229	25	0.78 ± 0.02	—
	214	10	0.69 ± 0.01	—
$Co(NH_2Me)_5OH_2^{3+}$	254	10	0.70 ± 0.01	0.49 ± 0.03
$Co(NH_2Pr)_5OH_2^{3+}$	254	10	0.54 ± 0.05	0.35 ± 0.01

[a]Quantum yield of Co^{2+} production measured in pH ~3.2 aqueous solution.
[b]Error limits represent mean deviation of two or more determinations.
[c]Not determined.

production can be estimated from eqn. (15). Using the $\phi_{Co^{2+}}$ values determined at 254 nm, we find that 64% of the Co^{2+} originates from the photoredox process (eqn. (13)) and 36% results from the thermal reaction (eqn. (14)).

$$Co(NH_2Me)_6^{3+} \xrightarrow{h\nu} Co_{(aq)}^{2+} + 5NH_2Me + {}^{\cdot+}NH_2Me \quad (13)$$

$$Co(NH_2Me)_6^{3+} + \cdot NH_2CH_2 \rightarrow Co_{(aq)}^{2+} + 6NH_2Me + \text{other products} \quad (14)$$

$$\%\ Co^{2+}\ \text{formed photochemically} = 1 - \left(\frac{\phi_{Co^{2+}}\ (\text{in Ar})}{\phi_{Co^{2+}}\ (\text{in air})}\right) \times 100 \quad (15)$$

Several observations support the foregoing explanation of the oxygen effect. First, the NH_2Me/Co^{2+} product ratio increases in deoxygenated solution (Table 5). This behavior reflects the contribution of the thermal reduction process (eqn. (14)), which liberates six moles of free amine compared with only five moles in the photochemical step (eqn. (13)). Second, the rise in pH of a photolyzed solution is less than predicted based upon the number of moles of methylamine released. This disparity can be ascribed to reactions of ${}^{\cdot+}NH_2Me$ and $\cdot NH_2CH_2$ that liberate protons (eqn. (16)) [27]. Finally, analysis of the photolyte reveals the presence of significant amounts of formaldehyde (Table 5), the expected product of $\cdot NH_2CH_2$ oxidation by $Co(NH_2Me)_6^{3+}$ or O_2 (eqn. (16)). The smaller CH_2O/Co^{2+} product ratio measured in deoxygenated solution is a consequence of the extra Co^{2+} produced via thermal reduction of the complex. Upon subtracting this thermal contribution

TABLE 5

Product ratios for photoredox reactions of (methylamine)cobalt(III) complexes[a]

Complex	λ_{excit} (nm)	NH_2Me/Co^{2+} [b]		CH_2O/Co^{2+} [c]	
		Ar purged	Air-equilibrated	Ar purged	Air-equilibrated
$Co(NH_2Me)_6^{3+}$	254	5.89 ± 0.13[d]	5.20 ± 0.07	0.42 ± 0.01	0.64 ± 0.01
	229	—[e]	—	0.40 ± 0.01	0.62 ± 0.03
$Co(NH_2Me)_5Br^{2+}$	366	—	—	0.04 ± 0.01	—
	313	—	—	0.08 ± 0.01	0.10 ± 0.01
	254	5.02 ± 0.40	5.02 ± 0.35	0.14 ± 0.02	0.21 ± 0.02
	229	—	—	0.20 ± 0.03	0.26 ± 0.01
$Co(NH_2Me)_5Cl^{2+}$	313	—	—	0.37 ± 0.02	0.40 ± 0.02
	254	4.91 ± 0.07	4.30 ± 0.20	0.38 ± 0.01	0.51 ± 0.02
	229	—	—	0.41 ± 0.01	0.59 ± 0.04

[a] Determined in pH ~3.2 aqueous solution at 10.0°C.
[b] Ratio of (mol NH_2Me) to (mol Co^{2+}) in photolyte.
[c] Ratio of (mol CH_2O) to (mol Co^{2+}) in photolyte.
[d] Error limits represent mean deviation of two or more values.
[e] Not determined.

(36% of the total Co^{2+}) and recalculating the ratio, we obtain a value experimentally indistinguishable from the one measured in the presence of oxygen. This interesting finding suggests that $Co(NH_2Me)_6^{3+}$ and O_2 oxidize $\cdot NH_2CH_2$ to CH_2O with comparable chemical yields.

$$^{\cdot+}NH_2Me \xrightleftharpoons{-H^+} \cdot NH_2CH_2 \xrightarrow{-e} CH_2=NH_2^+ \xrightarrow[-H^+]{H_2O} CH_2O + NH_3 \quad (16)$$

Irradiation of $Co(NH_2Me)_5OH_2^{3+}$ and $Co(NH_2Pr)_5OH_2^{3+}$ at 254 nm induces redox decomposition from the N→Co CT excited state (eqn. (17)). While detailed mechanistic studies were not undertaken, the larger $\phi_{Co^{2+}}$ values measured in deoxygenated solution (Table 4) are entirely consistent with the production of $^{\cdot+}NH_2R$ in the primary photochemical step.

$$Co(NH_2R)_5OH_2^{3+} \xrightarrow{h\nu} Co_{(aq)}^{2+} + 4NH_2R + {}^{\cdot+}NH_2R \quad (17)$$

3.2.2 $Co(NH_2Me)_5Br^{2+}$

The redox photochemistry of $Co(NH_2Me)_5Br^{2+}$ displays a complexity that can be understood in terms of contributions from two orbitally distinct LMCT excited states. Excitation at 229 nm populates the higher-energy N→Co CT state (Fig. 3) and leads to redox decomposition with characteristics similar to those observed for $Co(NH_2Me)_6^{3+}$. Thus $\phi_{Co^{2+}}$ is relatively independent of temperature but decreases in the presence of oxygen (Table 6). Moreover, formaldehyde is detected among the photoproducts (Table 5). We infer from these findings that formation of the $^{\cdot+}NH_2Me$ cation radical occurs directly from the N→Co CT excited state (eqn. (18a)). In contrast, values of $\phi_{Co^{2+}}$ determined at excitation wavelengths $\geq$254 nm generally exhibit little dependence upon oxygen but increase with increasing temperature (Table 6). Analysis of the photolyte establishes the stoichiometric relationship (mol NH_2Me) = 5(mol Co^{2+}), independent of oxygen concentration (Table 5). Flash photolysis experiments ($\lambda_{exit} > 250$ nm) conducted on N_2-bubbled solutions containing 0.1 M Br^- reveal the formation of $Br_2^{-\cdot}$, the expected product of the reaction between $Br\cdot$ and Br^- [28,29]. Formaldehyde is again found as a photoproduct but in amounts that decrease with increasing excitation wavelength (Table 5); possibly, oxidation of free NH_2Me or NH_3Me^+ by $Br\cdot$ contributes to CH_2O production at longer wavelengths [30]. Collectively, these results indicate that the redox chemistry occurring at wavelengths $\geq$254 nm originates from the Br→Co CT excited state (eqn. (18b)), with little or no contribution from the N→Co CT state.

$$Co(NH_2Me)_5Br^{2+} \xrightarrow{h\nu} \begin{cases} \xrightarrow{N\rightarrow Co} Co_{(aq)}^{2+} + 4NH_2Me + {}^{\cdot+}NH_2Me + Br^- & (18a) \\ \xrightarrow[Br\rightarrow Co]{} Co_{(aq)}^{2+} + 5NH_2Me + Br\cdot & (18b) \end{cases}$$

TABLE 6
Photoredox quantum yield data for $Co(NH_2Me)_5Br^{2+}$

λ_{excit} (nm)	Temp. (°C)	$\phi_{Co^{2+}}$[a]	
		Ar purged	Air-saturated
405	10	0.10 ± 0.01[b]	—[c]
366	10	0.17 ± 0.01	—
334	10	0.23 ± 0.01	—
313	5	0.21 ± 0.01	—
313	10	0.32 ± 0.02	0.31 ± 0.01
313	15	0.30 ± 0.03	—
313	25	0.37 ± 0.02	0.39 ± 0.01
290	10	0.39 ± 0.02	—
254	5	0.37 ± 0.01	—
254	10	0.43 ± 0.01	0.38 ± 0.03
254	15	0.48 ± 0.01	—
254	25	0.55 ± 0.02	0.52 ± 0.01
229	5	0.55 ± 0.01	—
229	10	0.59 ± 0.03	0.49 ± 0.01
229	15	0.58 ± 0.01	—
229	25	0.71 ± 0.01	—
214	10	0.56 ± 0.02	—

[a]Quantum yield of Co^{2+} production measured in pH ~3.2 aqueous solution.
[b]Error limits represent mean deviation of two or more determinations.
[c]Not determined.

Figure 4 depicts the quantum yield vs. excitation wavelength profiles for $Co(NH_2Me)_5Br^{2+}$ in different solvents. In water, $\phi_{Co^{2+}}$ increases monotonically with decreasing excitation wavelength within the range 405–254 nm and appears to approach a limiting value (broken line) characteristic of reaction from a bound state. Arguments presented above support the view that this state is Br → Co CT in character (eqn. (18b)). More specifically, the quantum yield in the vicinity of 250 nm most likely corresponds to reaction from the Br(σ) → Co CT state, whereas the drop in $\phi_{Co^{2+}}$ at longer wavelengths may represent an increasing contribution from a less reactive Br(π) → Co CT state. The abrupt rise in $\phi_{Co^{2+}}$ to a new plateau at excitation wavelengths below 250 nm signals the occurrence of a second redox reaction originating from the higher-lying N → Co CT excited state (eqn. (18a)). The alternative explanation, in which the initially populated N → Co CT state crosses to a dissociative CT state arising from the transfer of an electron from a solvent molecule to the complex (see, for example, eqn. (9)) can be discounted by the results obtained in mixed-solvent systems (Fig. 4). Thus, unlike the behavior of the $Co(NH_3)_5X^{2+}$ family, the qualitative features of the quantum yield profile in water are retained in both 80% acetonitrile and 50% glycerol solutions. Particularly noteworthy is the absence

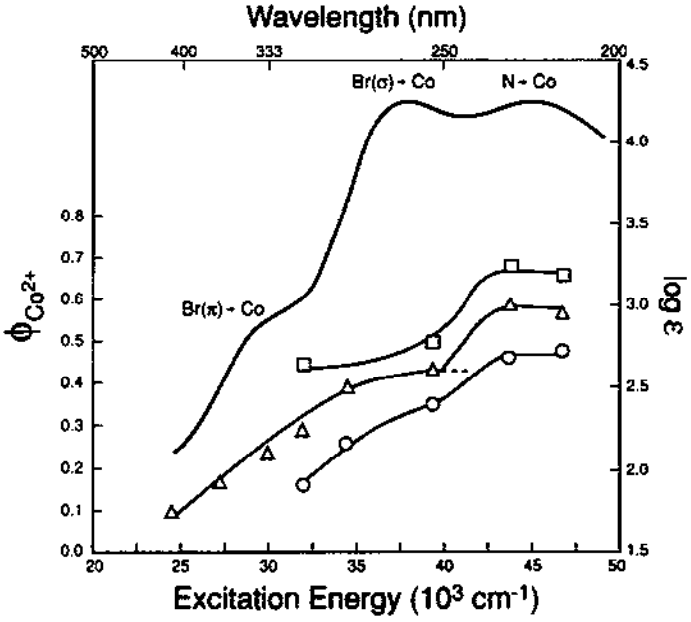

Fig. 4. Absorption spectrum (uppermost curve) of $Co(NH_2Me)_5Br^{2+}$ in water at 10°C and quantum yield profiles (lower curves) for photoredox decomposition of $Co(NH_2Me)_5Br^{2+}$ in various solvent media: △, water; □, 80% acetonitrile–water; ○, 50% glycerol–water. All solutions were deoxygenated and contained 10^{-3} M $HClO_4$. (Reproduced from ref. 15. Copyright 1991 American Chemical Society.)

of photodissociative character (i.e. a continuous rise in $\phi_{Co^{2+}}$ toward unity) at high excitation energies in these mixed solvents. Interestingly, the values of $\phi_{Co^{2+}}$ at a specific wavelength vary with solvent in the order 80% acetonitrile > water > 50% glycerol. This trend tracks solution viscosity and suggests that solvent influences the photoredox chemistry of $Co(NH_2Me)_5Br^{2+}$ largely through its effect upon the separation/recombination kinetics of primary (eqns. (2) and (3)) and secondary (eqns. (4) and (6)) radical-pair photoproducts.

3.2.3 *$Co(NH_2Me)_5Cl^{2+}$, $Co(NH_2Et)_5Cl^{2+}$, and $Co(NH_2Pr)_5Cl^{2+}$*

It was noted earlier that the single absorption band displayed by $Co(NH_2R)_5Cl^{2+}$ complexes (see, for example, Fig. 2) is composed of overlapping $N \rightarrow Co$ and $Cl(\sigma) \rightarrow Co$ CT transitions. Selective excitation of the methylamine complex at various wavelengths within this band leads to two distinctly different photochemical responses. Irradiation at 229 or 254 nm induces redox decomposition with $\phi_{Co^{2+}}$ values that show little dependence upon temperature but decrease in the presence of oxygen (Table 7). Oxygen also causes a drop in the NH_2Me/Co^{2+} product ratio determined at 254 nm (Table 5). Formaldehyde is detected in the photolyte, and the CH_2O/Co^{2+} ratio is enhanced by the presence of oxygen (Table 5). As discussed in detail for $Co(NH_2Me)_6^{3+}$ and $Co(NH_2Me)_5Br^{2+}$, these characteristics

TABLE 7
Photoredox quantum yield data for $Co(NH_2R)_5Cl^{2+}$

Complex	λ_{excit} (nm)	Temp. (°C)	$\phi_{Co^{2+}}$[a]	
			Ar purged	Air-saturated
$Co(NH_2Me)_5Cl^{2+}$	313	5	0.23 ± 0.01[b]	—[c]
	313	10	0.29 ± 0.01	0.29 ± 0.01
	313	25	0.36 ± 0.02	0.37 ± 0.02
	290	10	0.34 ± 0.03	—
	254	5	0.52 ± 0.01	—
	254	10	0.54 ± 0.02	0.40 ± 0.02
	254	25	0.59 ± 0.05	0.40 ± 0.02
	229	5	0.63 ± 0.02	—
	229	10	0.63 ± 0.01	0.46 ± 0.01
	229	25	0.65 ± 0.01	—
	214	10	0.62 ± 0.01	—
$Co(NH_2Et)_5Cl^{2+}$	313	10	0.24 ± 0.01	—
	254	10	0.51 ± 0.04	0.39 ± 0.02
	254	25	0.49 ± 0.02	0.38 ± 0.01
	229	5	0.49 ± 0.01	—
	229	10	0.44 ± 0.02	—
$Co(NH_2Pr)_5Cl^{2+}$	313	10	0.20 ± 0.01	—
	254	10	0.49 ± 0.04	0.35 ± 0.02
	254	25	0.48 ± 0.01	0.35 ± 0.05
	229	5	0.48 ± 0.01	—
	229	10	0.45 ± 0.01	—

[a] Quantum yield of Co^{2+} production measured in pH ~3.2 aqueous solution.
[b] Error limits represent mean deviation of two or more determinations.
[c] Not determined.

are diagnostic of reaction occurring from the higher-lying N→Co CT excited state (eqn. (19a)).

$$Co(NH_2Me)_5Cl^{2+} \xrightarrow{h\nu} \begin{cases} \xrightarrow{N\rightarrow Co} Co^{2+}_{(aq)} + 4NH_2Me + {}^{\cdot+}NH_2Me + Cl^- & (19a) \\ \xrightarrow{Cl\rightarrow Co} Co^{2+}_{(aq)} + 5NH_2Me + Cl^- & (19b) \end{cases}$$

Excitation at 313 nm, which corresponds to the long-wavelength tail of the composite absorption band, causes redox decomposition characterized by $\phi_{Co^{2+}}$ values that exhibit no oxygen dependence but increase with increasing temperature (Table 7). Formaldehyde is again detected among the photoproducts, although the

CH_2O/Co^{2+} ratio does not depend upon oxygen (Table 5). We attribute these results to a reaction originating from the $Cl(\sigma) \rightarrow Co$ CT excited state (eqn. (19b)).

Flash photolysis experiments ($\lambda_{exc} > 240$ nm) conducted on N_2-bubbled solutions containing 0.01 M Cl^- failed to detect $Cl_2^{-\cdot}$, the expected product of reaction between $Cl\cdot$ and Cl^- [6,29]. It appears, therefore, that photogenerated $Cl\cdot$ undergoes a very rapid (within 100 ns) reaction with another species in the system. An attractive possibility is oxidation of a NH_2Me ligand present in the original coordination sphere [31]. This reaction also could account for the appreciable CH_2O generated at 313 nm, although it would be necessary to postulate that this process is unaffected by O_2.

Less detailed studies of the photoredox reactions of $Co(NH_2Et)_5Cl^{2+}$ and $Co(NH_2Pr)_5Cl^{2+}$ were undertaken. To the extent that comparisons can be made (Table 7), however, it appears that these complexes behave similarly to their methylamine analogue.

3.3 Mechanistic implications

The preceding results establish that $Co(NH_2Me)_5Br^{2+}$ and $Co(NH_2Me)_5Cl^{2+}$ (and probably $Co(NH_2Et)_5Cl^{2+}$ and $Co(NH_2Pr)_5Cl^{2+}$) possess two photoactive LMCT excited states which undergo poor communication with one another. Preferential population of the $N \rightarrow Co$ CT state at shorter excitation wavelengths leads to the production of nitrogenous radicals (eqns. (18a) and (19a)) that can be scavenged by O_2, whereas longer-wavelength irradiation favors population of the lower-energy $Br \rightarrow Co$ or $Cl \rightarrow Co$ CT state, which favors redox chemistry (eqns. (18b) and (19b)) unaffected by O_2. The characteristic reactions of these two types of CT states also respond very differently to changes in temperature. Figure 5 displays apparent activation energies, E_a, as a function of excitation wavelength; the E_a values were calculated from Arrhenius-type plots of $\ln(\phi_{Co^{2+}})$ vs. $1/T$. Reactions which originate from the $N \rightarrow Co$ CT state possess apparent activation energies between 0–1 kcal mol^{-1}. This group encompasses the photoredox decompositions of $Co(NH_2Me)_6^{3+}$ at 229 and 254 nm, $Co(NH_2Me)_5Br^{2+}$ at $\leqslant 229$ nm, and $Co(NH_2Me)_5Cl^{2+}$ at $\leqslant 254$ nm. Reactions occurring from the $Br \rightarrow Co$ or $Cl \rightarrow Co$ CT state are more sensitive to temperature, with E_a values falling in the 3–5 kcal mol^{-1} range. Included in this group are the redox processes observed for $Co(NH_2Me)_5Br^{2+}$ at $\geqslant 254$ nm and $Co(NH_2Me)_5Cl^{2+}$ at 313 nm. That E_a rises for the bromo complex between 254 and 313 nm may reflect different temperature dependencies of reactions from the $Br(\sigma) \rightarrow Co$ and $Br(\pi) \rightarrow Co$ CT excited states.

As noted in the Introduction, there have been no reports of redox chemistry occurring from the $N \rightarrow Co$ CT excited state of $Co(NH_3)_5X^{2+}$ complexes. Instead, this state undergoes efficient internal conversion to the lower-lying $X \rightarrow Co$ CT state and/or crossing to a dissociative solvent $\rightarrow Co$ CT state. Evidently, replacement of NH_3 by NH_2R alters the behavior of the $N \rightarrow Co$ state such that chemical reaction

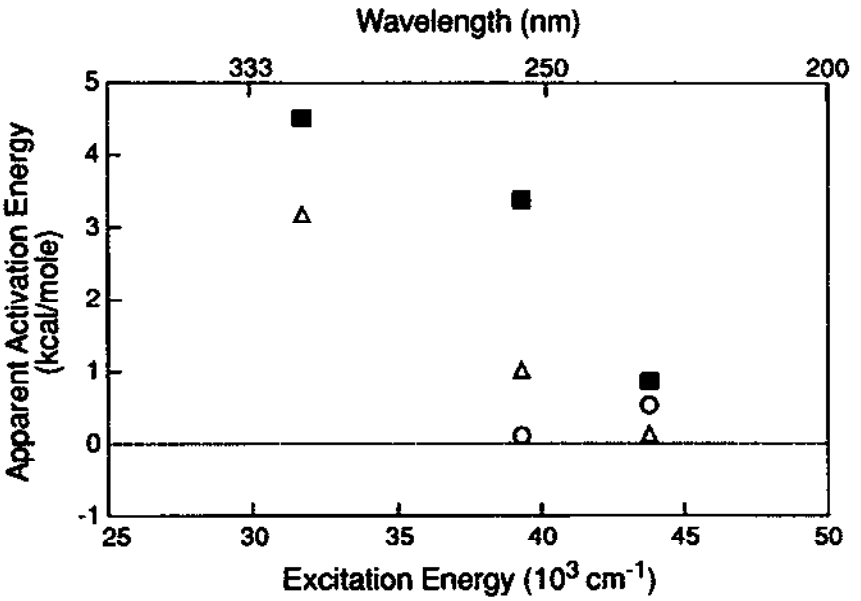

Fig. 5. Apparent activation energies for photoredox decomposition of (methylamine)cobalt(III) complexes as a function of excitation energy: ○, $Co(NH_2Me)_6^{3+}$; △, $Co(NH_2Me)_5Cl^{2+}$; ■, $Co(NH_2Me)_5Br^{2+}$.

increases in importance relative to other relaxation processes. Two explanations for this ligand effect have been suggested [14]. (1) The hydrophobic alkyl groups situated on the periphery of alkylamine complexes reduce dielectric and/or hydrogen bonding interactions with the surrounding solvent. One consequence of this decreased solvation is a lowering of the reorganizational barrier that must be surmounted during dissociation of the primary radical pair. (2) The N → Co CT excited state in alkylamine complexes possesses weaker Co—N bonds. This factor should favor intramolecular decomposition over crossing to the potential energy surfaces of other CT states.

It is difficult to reconcile the first explanation with the similar solvatochromic shifts experienced by the Br(σ) → Co CT transitions in $Co(NH_3)_5Br^{2+}$ and $Co(NH_2Me)_5Br^{2+}$ (compare ΔE values in Table 3). We would expect smaller shifts for the latter complex if its methyl groups were effective in reducing interactions with the solvent. A stronger case can be made for the second explanation. While complexes belonging to both families undergo metal–ligand bond labilization in their LMCT states resulting from population of σ-antibonding orbitals, there is the possibility of additional bond weakening in the alkylamine systems arising from nonbonded repulsions between the bulky (relative to H) alkyl groups. [32,33]

4. CONCLUDING REMARKS

Comparison of the ultraviolet photoreactivities of analogous ammine and alkylamine complexes of cobalt(III) reveals several similarities. Both families undergo

efficient photoredox decomposition from LMCT excited states. The primary photoproduct in each case is a radical pair, which, in subsequent steps, either recombines or reacts further to yield the final products. Solvent can influence the observed reactivity through its effect upon the LMCT excited state energy, the kinetics of radical pair separation/recombination, and the subsequent reactions of photogenerated radicals. Despite these similarities and the implied commonality of mechanism, there are some important and previously unanticipated differences in behavior between the two families of complexes. Thus only members of the $Co(NH_2R)_5X^{2+}$ family undergo intramolecular redox reactions from the higher-lying $N \rightarrow Co$ CT excited state. Moreover, the high reactivity of this state in alkylamine complexes effectively precludes it from crossing to a dissociative solvent $\rightarrow$ Co CT state. These differences demonstrate that nominally modest modifications in ligand structure (replacement of H by CH_3) can cause significant changes in LMCT excited-state reactivity.

ACKNOWLEDGMENTS

Financial support for this work was provided by the National Science Foundation, the IBM Corp., and the Office of Basic Energy Sciences of the Department of Energy. This is contribution NDRL-3551 from the Notre Dame Radiation Laboratory.

REFERENCES

1 V. Balzani and V. Carassiti, Photochemistry of Coordination Compounds, Academic Press, New York, 1970, Chap. 11.
2 J.F. Endicott, in A.W. Adamson and P.D. Fleischauer (Eds.), Concepts of Inorganic Photochemistry, Wiley-Interscience, New York, 1975, Chap. 3.
3 J.F. Endicott, G.J. Ferraudi and J.R. Barber, J. Phys. Chem., 79 (1975) 630.
4 C. Kutal and A.W. Adamson, in G. Wilkinson, R.D. Gillard and J.A. McCleverty (Eds.), Comprehensive Coordination Chemistry, Vol. 1, Pergamon Press, New York, 1987, Chap. 7.3.
5 G.J. Ferraudi, Elements of Inorganic Photochemistry, Wiley-Interscience, New York, 1988, Chap. 5.
6 J. Lilie, J. Am. Chem. Soc., 101 (1979) 4417.
7 J.F. Endicott, G.J. Ferraudi and J.R. Barber, J. Am. Chem. Soc., 97 (1975) 219.
8 M. Orhanovic and N. Sutin, Inorg. Chem., 16 (1977) 550.
9 C.H. Langford and E. Lindsay, Inorg. Chem., 29 (1990) 1450.
10 G.J. Ferraudi, J.F. Endicott and J.R. Barber, J. Am. Chem. Soc., 97 (1975) 6406.
11 C. Kutal and C.G. Willson, J. Electrochem. Soc., 134 (1987) 2280.
12 C. Kutal, S.K. Weit, S.A. MacDonald and C.G. Wilson, J. Coating Technol., 62 (1990) 63.
13 S.K. Weit, C. Kutal and R.D. Allen, Chem. Mater., 4 (1992) 453.
14 S.K. Weit and C. Kutal, Inorg. Chem., 29 (1990) 1455.
15 S.K. Weit, P.A. Grutsch and C. Kutal, Inorg. Chem., 30 (1991) 2819.
16 Y.N. Shevchenko and N.B. Golub, Russ. J. Inorg. Chem. (Engl. Transl.), 24 (1979) 1689.

17 S.C. Chan and K.Y. Hui, Aust. J. Chem., 20 (1967) 2529.
18 L.F. Book, K.Y. Hui, O.W. Lau and W.-K. Li, Z. Anorg. Allg. Chem., 426 (1976) 215.
19 R. Mitzner, P. Blankenburg and W. Depkat, Z. Chem., 9 (1969) 68.
20 C.A. Koval and M.E. Ketterer, J. Electroanal. Chem., 175 (1984) 263.
21 C.G. Hatchard and C.A. Parker, Proc. R. Soc. (London) Ser. A, 235 (1956) 518.
22 D.R. Prasad and G. Ferraudi, Inorg. Chem., 21 (1982) 4241.
23 F. Vydra and R. Pribil, Talanta, 5 (1960) 44.
24 S. DeBernado, M. Weigele, V. Toome, K. Manhart, W. Leimgruber, P. Böhlen, S. Stein and S. Udenfriend, Arch. Biochem. Biophys., 163 (1974) 390.
25 S.A. Schmidt, M.F. Antloga and M. Markelov, Formaldehyde: Analytical Chemistry and Toxicology, American Chemical Society, Washington, DC, 1985, Chap. 3.
26 H.-H. Schmidtke, in H.O.A. Hill and P. Day (Eds.), Physical Methods in Advanced Inorganic Chemistry, Interscience, London, 1968, Chap. 4.
27 C.K. Mann and K.K. Barnes, Electrochemical Reactions in Nonaqueous Systems, Dekker, New York, 1970, Chap. 9.
28 M. Schöneshöfer and A. Henglein, Ber. Bunsenges. Phys. Chem., 73 (1969) 289.
29 G.J. Ferraudi, Elements of Inorganic Photochemistry, Wiley-Interscience, New York, 1988, Chap. 2.
30 S.A. Penkett and A.W. Adamson, J. Am. Chem. Soc., 87 (1965) 2514.
31 G. Caspari, R.G. Hughes, J.F. Endicott and M.Z. Hoffman, J. Am. Chem. Soc., 92 (1970) 6801.
32 T.W. Swaddle, Can. J. Chem., 55 (1977) 3166.
33 B.M. Foxman, Inorg. Chem., 17 (1978) 1932.
34 L.F. Book, K.Y. Hui, O.W. Lau and W.-K, Li. Z. Anorg. Allg. Chem., 426 (1976) 227.